博 士 論 文

Characterization of minocycline-carbon nanohorn conjugates and their antibacterial activity

（ミノサイクリン - カーボンナノホーンの複合体の製作ならびにその静菌効果について）

令和２年３月申請

北海道大学

大学院歯学研究科口腔医学専攻

前　田　由　佳　利

Introduction

The unique characteristics of carbon nanomaterials such as graphene, carbon nanotubes (CNTs) and carbon nanohorns (CNHs) make them ideal candidates for research into their biomedical applications. [1–9] They have been found to be particularly effective in applications for bone tissue engineering because of their cytocompatibilty, mechanical, and electrical properties. [10–13] In a previous study we reported that osteoblast adhesion and differentiation could be enhanced by CNT-coated substrates, while sponges coated with CNTs showed a high level of biocompatibility with bone. [14–18]

Among carbon nanomaterials, there is currently a great interest in creating biomedical applications using CNHs. CNHs have an irregular shape of 2-5 nm in diameter and 40-50 nm in length. Thousands come together to form a spherical assembly of approximately 100 nm in diameter. [19] High biocompatibility has been reported [20–22] because no metal catalyst is used. [23] For cannular CNT, the aspect ratios (or length/wide ratios) as the key factor significantly affect their toxicity, while SNH are approximately isotropic in three dimensions owing to the spherical morphology. [24][25] Moreover, because of the formation of nano-windows on the walls by combustion, carbon nanohorns become porous, and the area of adsorption is about four times. In addition, by changing the conditions of oxidation, it is possible to control the size and number of pores. [26][27] This function is commonly used to hold drugs such as cisplatin and hydrochloride vancomycin. [28][29]

Previously, we have concentrated on CNHs and osteogenesis and documented enhancing osteogenesis on the CNH membrane [30] and promoting osteoblast differentiation by macrophages integrating CNHs. [31] This feature is expected to be applied to the surface modification of dental implants. In patients who have lost their teeth, dental implants are an effective therapy. [32][33] On the other hand, peri-implantitis is well known as inflammation caused by the implant's bacterial

infection. While inflammation progresses, the implant-supporting bone tissue is absorbed, and the implant is lost. [34–36] Antibiotics are one of the treatments for peri-implantitis. Is a method by injecting an antibiotic around the suffering implant to suppress inflammation. [37] Minocycline (MC) is one of the widely used as antibiotic. [38] To maintain an effective concentration of the drug when administered systemically, high dose of MC is necessary. [39,40] Therefore, local delivery may be highly effective for the treatment of peri-implantitis. However, most of antibiotics run out of the implant and are difficult to keep for a long time. MC should be administered frequently to obtain a bacteriostatic effect without increasing local concentrations.

Therefore, we expected that the CNHs could be a carrier for applying in local delivery applications. In this study, we compared the difference with and without oxidation of CNHs in loading ability and bacteriostatic action. The effect on the osteoblast has also been verified.

Materials & Methods

General

Minocycline hydrochloride (MC) and other organic solvents were purchased from Fuji-film Wako Corp (Japan). CNHs were obtained from NEC Corp (Tokyo, Japan). CNHs were produced by CO_2 laser ablation of a pure-graphite target at room temperature in Ar gas at 760 Torr. [40] The purity of CNH used is about 95%, and most of the impurities of about 5% are graphitic spheres with amorphous structure. [41] No metal catalyst was used in this process. Air-oxidized CNHs were prepared by the reported procedure. CNHs were heated under air flow at the temperature increase rate 1 ° C / min, up to 550 ° C, then cooled under air flow. [42]

Preparation of MC/CNHs conjugates

One mg of MC was dissolved in 10.0 mL of deionized water to prepare a stock solution of MC. MC/CNHs conjugate was prepared by adding 1 mg of powdered as-grown CNHs (as-CNHs) or CNHs oxidized at 550 ^{o}C (CNHox550) into the MC solution in various concentration of MC (0, 20, 40, 60, 80, 100, 150 μg / mL of MC for 100 μg / mL of CNHs). The CNHs and MC solution was then subjected by ultrasonication in cold water (5 to 10 ° C) for 2 hrs. For bacterial and cell culture, the dispersion was added in the culture medium at the concentrations as described below.

Transmission electron microscopy observation

MC/CNHs immediately after fabrication were observed by HR-TEM (JEM-2010F, JEOL, Tokyo, Japan) with acceleration voltage of 200kv ,and STEM (Titan-cubed G2 60-300（FEI, Hillsboro, OR, USA）) with acceleration voltage of 80kv. For comparison, CNHs dispersed with 100% ethanol were also observed.

Absorption spectral measurements

Absorption spectra of MC, CNHs, and MC/CNHs were recorded by a Nanodrop UV–vis spectrophotometer

Nanodrop (Thermo™INSIGHT, ThemoFischer, Waltham, MA, USA).

Thermo Gravimeter & Differential Thermal Analysis (TG/DTA).

For the thermogravimetric analysis, the dispersion was lyophilized using a VD-400F (TAITEC, Saitama, Japan) and MC/CNHs was obtained as black powder. Thermogravimetric analysis was carried out using a TG 8120 Thermo Gravimeter & Differential Thermal Analysis (Rigaku Corporation, Tokyo, Japan). 2 mg of the sample was taken onto a platinum pan and the temperature was increased from room temperature to 1000 °C at a rate of 10 °C/min under N_2 flowing at 100 mL/ min.

Quantification of released MC

The released amount of MC from CNHs was quantified by using dialysis cassettes (Slide-A-Lyzer G2, MWCO 7k Da, ThemoFischer, Waltham, MA, USA). Dialysis cassettes containing 0.5 mL sample solutions were placed in 10mL of phosphate buffer solution (PBS (-), Wako, Osaka, Japan) at room temperature. An aliquot of 100 μL was taken out of each dialysis cassette at the time intervals of 1, 2, 5, 8 hrs, 1, 2, 3, and 7 days. The aliquots taken at each time point were analyzed by the UV–vis spectrophotometer at the absorbance of 350nm.

Bacterial culture

Streptcoccus mutans (ATCC 55677) was cultured in brain heart infusion (BHI; BD, Franklin Lakes, NJ, USA) medium, and *Aggregatibacter actinomycetemcomitans* (ATCC 29522) was cultured in

BHI medium with 1% yeast(Bacto™ Yeast Extract; BD, Franklin Lakes, NJ, USA). MC/CNHs dispersion was added to the culture medium so that the minocycline concentration was 0, 0.05, 0.1, 0.2, 0.4, 0.8 μg/mL, respectively.

The tube was incubated at 37 ° C in an atmosphere with 95% air and 5% CO_2. After 24 hours, the turbidity of the medium was measured by the absorbance at 600 nm (SmartSpec Plus, BIO-RAD, Hercules, CA, USA). The turbidity was divided by the absorbance at the time of bacterial seeding and the growth rate was confirmed.

TEM and SEM observationof bacterial

At 20 hours after bacteria culturing, the specimen for the observations by scanning electron microscopy (SEM) and TEM. For SEM observation, the bacterias were fixed with 2% glutaraldehyde. After dehydration through a graded ethanol series, they were dried using the critical point method and sputter coated with palladium-platinum for SEM observation (S-4800, HITACHI, Tokyo, Japan). For TEM observation, the bacterias were fixed with 1% OsO4 and embedded in epoxy resin after dehydration. The ultrathin sections were obtained using an ultramicrotome (Leica) with a diamond knife (DiATOME). The ultrathin sections were examined by TEM (JEM1400, 80 V) (JEOL, Tokyo, Japan).

Osteoblast cell culture

Mouse osteoblast MC3T3-E1 cells were suspended in general medium consisting of 6.67×10^4 cells/mL in minimum essential medium, alpha modification (a-MEM; Gibco, ThemoFischer, Waltham, MA, USA), containing 5 % fetal bovine serum (FBS; Biowest, Nuaillé , France), 100 units/mL penicillin, 100 μg/mL streptomycin, (Pen Strep; Gibco, France) and 5 μL/mL L-glutamine (Sigma-Aldrich, St. Louis, MO, USA). Three hundred microliters of the cell suspension was seeded

in each well of the 48-well plates. After 3 hours, the culture medium was then replaced to osteoblast differentiation medium consisting of with 50 μM ascorbic acid, 10 mM β-glycerophosphate with MC/as-CNH, MC/CNHox550 dispersions as mentioned above at the concentration of 0.8 μg/mL of MC.

After 7 days of cell culture, the amounts of DNA and ALP activities of the samples were measured. Each well was washed twice with PBS. Three hundred microliters of the cell suspension containing 0.2% IGEPAL CA630 (Sigma-Aldrich, St. Louis, MO, USA), 10 mM Tris-HCl and 1 mM $MgCl_2$, pH 7.4, was added to each sample. The samples were frozen, thawed and homogenized. The sample solution was added to 100 mL of 4 M NaCl, 0.1 M phosphate buffer (pH 7.4) and then centrifuged for DNA analysis. Picogreen (Molecular Probes, Leiden, Netherlands) was used to measure the DNA content by means of a microplate reader (infinite F200 PRO, TECAN, Kanagawa, Japan), with the excitation filter set at 365 nm and the emission filter at 450 nm. Alkaline phosphatase (ALP) activity was measured with LabAssay (Wako, Osaka, Japan) as described previously [31]. ALP activity was normalized by DNA content. The DNA content and ALP activity were determined in five samples. All data are presented ± standard error of the mean (SEM). Statistical analyses were performed using GraphPad Prism (GraphPad software, San Diego, CA, USA) and one-way ANOVA followed by Dunn's multiple comparisons test.

Results

1.Preparation of MC/CNHs conjugates

Absorbances at 600 nm were used to determine the dispersed CNHs concentration in PBS (Figure 1A) because MC does not show optical absorption longer than 500 nm. It was found that the sonication of CNHs with MC remarkably increased the absorbance at 600 nm, which indicates the better dispersion of CNHs in the solution (Figure 1B). The dispersion solutions are stable longer than 1 hr. In the condition using 60 μg/mL of MC, absorbance at 600 nm of as-CNHs increased 4 times relative to that without the treatment of MC (Figure 1C, D). CNHox550 also showed a remarkable increase of the absorbance at 600 nm after with the treatment of MC, although CNHox550 without MC-treatment showed relatively high absorbance.

In absorption spectra, MC shows a characteristic absorption band around 345 nm. MC/CNHs conjugates showed the characteristic peak of MC whose intensity increase with the concentration of MC (Figure 2A). Notably, MC concentrations below 20 μg/mL and 80 μg/mL in the cases of MC/as-CNH and MC/CNHox550, respectively, do not show characteristic absorption bad of MC (Figure 2B).

Thermogravimetric analyses (TGA) were performed in N_2 atmosphere to confirm the thermodynamic detachment of decomposition of MC on the CNHs. For pure MC, a large weight loss was observed around 230 ºC, which would be assigned to the vaporization or decomposition of MC, whereas the both pristine CNHs (as-CNHs and CNHox550) alone showed almost no weight loss around 230 ºC (Figure 3). In contrast, as-CNHs and CNHox550 which were treated with MC demonstrated remarkable weight loss around 230 ºC. Moreover, the reduction rates of weight in the both case of as-CNHs and CNHox550 were larger than those of MC-untreated CNHs at higher temperature than 500 ºC, suggesting the decomposition of MC on the CNHs. It is also worth mentioning that the weight loss of MC/as-CNH at the temperature higher than 600 ºC is much larger

than that of MC/CNHox550.

TEM observation of MC/CNH. Figure 4 A-D showed the MC/as-CNH, figure 4 E-H showed the MC/CNHox550. Figure 4A, E shows well-defined, especially figure 4E has a hole at the tip of the left horn. Figure 4B, F confirmed that there were many deposits around the horn structure in MC/CNHs in 200 kV TEM. 80kV HRTEM confirmed thread-like deposits around the horn (figure 4C, G). In STEM, MC/CNHox550 was unclear (figure 4D), but MC/as-CNH was confirmed that there were white spots seemed to be MC (figure 4H).

2. Sustained release of MC

MC-releasing abilities of MC/CNHs conjugates were examined by dialysis. This assay allows us to determine the amount of thermodynamically detached MC from CNHs into the solution with time. Absorption spectra of the recovered components by the dialysis were recorded and the optical absorbance at 350 nm were picked as the detached amount of MC from the CNHs. A control experiment was performed with using pure MC in the absence of CNHs (Figure 5). Pure MC alone showed quick elution from the container of dialysis, which was almost completed (~95 % relative to the amount after 7days) within 24 hrs. This rate is a typical rate to go through the cellulose membrane of the dialysis tube. Using the same amount of MC, MC/as-CNH and MC/CNHox550 showed 71 % and 55 % elution, respectively, relative to those after 7 days after 24 hrs. In comparing with the pure MC, MC/as-CNH released 62 % of MC after 7 days of dialysis, whereas MC/CNHox550 released 22 % of MC.

3. Bacterial culture

Figure 6 shows the growth rate of *A.a.* (Figure 6A) and *S.m*. (Figure 6B). MC at the concentration of 0.1 μg/mL or more showed bacteriostatic effect against *A.a.* The same concentration of MC/as-CNH

also suppressed bacterial growth, whereas MC/CNHox550 at the concentration of less than 0.4 μg/mL didn't show bacteriostatic effect. Similarly, the growth of *S.m.* was inhibited in the presence of MC or MC/as-CNH at the concentration of 0.4 μg/mL or more, while more than 0.8 μg/mL MC/CNHox550 show bacteriostatic effect.

In the SEM observation (Figure 7A, B), CNHs were observed to surround dead *A.a.*(Figure 7B). By TEM observation (Figure 7C-F), the cell wall of *A.a* cultured with MC was collapsed (Figure 7D). Moreover, Some CNHs were observed by TEM to touch the cell walls of dead bacteria (Figure 7E, F).

4. Osteoblast proliferation and differentiation

The DNA content and ALP activity of the cells cultivated for 7 days are shown in Figure 8. Compared in the absence of MC and CNHs as control, DNA content and ALP activity normalized to the DNA content with MC, as-CNHs, CNHox550, MC/as-CNH, MC/CNHox550 showed no significant differences ($p > 0.1$). There are also no significant differences between with MC and the groups of with CNHs.

Discussion

As-prepared CNHs are known to be water-insoluble, and thus a dispersant or applying chemical modifications are required to solubilize CNHs in aqueous solution. [28] In the present study, it was found that the sonication of CNHs with MC remarkably improves the CNHs concentration in water with such a simple and facile adsorption method. In the condition using 60 μg/mL of MC, the remarkable increase of absorbance at 600 nm indicated that the concentration of as-CNHs in the solution increased 4 times relative to that without using MC. Even though the oxidized-CNHs (CNHox550) is dispersible without any treatment because CNHox550 contains many of carboxylic groups which improve water-solubility of CNHs[40-42], MC can further improve the water dispersibility of CNHox550 significantly. These results also suggest that MCs adhere directly to CNHs and acts as a suitable dispersant for solubilizing CNHs in the aqueous solution.

The absorption spectra of MC/CNHs in the condition using different concentrations of MC to make the conjugate gave insight for the attachment mode of MC on or in the CNHs. MC concentrations below 40 μg/mL and 80 μg/mL in the cases of MC/as-CNH and MC/CNHox550, respectively, do not show remarkable absorption band of MC. This result suggests that MC adhered on CNHs strongly. The strong attachment causes broadening of the MC peak probably due to the strong electronic interaction between MC and CNHs. The MC absorption band was only detectable over a certain threshold of concentration (40 μg/mL and 80 μg/mL for MC/as-CNH and MC/CNHox550, respectively). This fact indicates that MC is, at least, in two different circumstances in which MC strongly adheres or relatively weakly attach on the CNHs.

TGA profiles demonstrated the different situations of MC among pure MC, MC/as-CNH, and MC/CNHox550. Weight loss around 230 ºC in MC/as-CNH, and MC/CNHox550 suggests the loss of relative free or weekly attached MC by heating. Because this loss is larger in MC/as-CNH than that in MC/CNHox550, it can be concluded that MC/as-CNH has such MC more than

MC/CNHox550. The weight loss of MC/as-CNH at the temperature higher than 500 ºC is also much larger than that of MC/CNHox550. It may be explained by the fact that MC can locate inside the CNHs. It is reported that the oxidation of CNHs makes it porous [26][27], and more amount of MC can be involved in the CNHs in the case of MC/CNHox550. And this involvement protects the inside MC from the thermal detachment/decomposition, which is more probable in CNHox550 than as-CNH.

Consequently, the lost amount of MC of MC/as-CNH at higher than 500 ºC is larger than that of MC/CNHox550.

MC-releasing abilities of MC/as-CNH and MC/CNHox550 were examined by the dialysis experiments. By comparing the optical absorbance at 350 nm, which is a characteristic band of MC, between that after 24 hrs and 7days, MC/as-CNH and MC/CNHox550 showed 71 % and 55 % of releases at 24 hrs. In the viewpoint of sustained-release of MC, MC/CNHox550 may be preferable than MC/as-CNH. MC/as-CNH and MC/CNHox550 showed different elution rates and amounts of MC each other. MC/as-CNH released 62 % of MC relative to the pure MC, whereas MC/CNHox550 released 22 % of MC after 7 days of dialysis. These results can be rationalized by the different manners of attachment of MC on the CNH as mentioned above. That is, MC may be in three different circumstances, which are on the surface of CNHs with strong interaction disappearing characteristic absorption band of MC, on the surface with relatively week interaction as observed in TGA around 230 ºC, or in the CNHs in the case using CNHox550. Based on this difference, it is expected that MC/as-CNH can distribute more amount of MC to the surrounding environment than MC/CNHox550, and probably the released MC is effective to bacteria.

To apply MC/CNHs for peri-implantitis, it is necessary to confirm that re-osseointegration after healing of peri-implant inflammation is not inhibited by MC/CNHs. In this study, the effect on the initial differentiation and proliferation of osteoblasts was examined by ALP activity which is an early

marker of osteoblastic cell differentiation.[43] In this study, MC/CNH and MC at which concentration was effective against bacteria didn't affect the cell differentiation and proliferation while Park et al. reported higher density of MC such as more than 100 μM led to a dose-dependent decrease of cellular differentiation and protein expression [39]. Besides, the presence of CNHs didn't show negative effect on osteoblasts. This result supports our previous report indicating that, the ALP activity of human mesenchymal stem cells did not change with CNHs.[31]

For *in vivo* toxicological assessments of CNHs, Miyawaki et al. reported that the CNHs was found to be a nonirritant and nondermal sensitizer through skin primary and conjunctival discomfort tests and skin sensitization examination. Intratracheal instillation tests revealed that for a 90-day test period, SWNHs rarely weakened rat lung tissue, while black pigmentation was observed due to accumulated CNHs. [22] In addition, we have reported that CNHs have high compatibility with bone tissue. [30] Moreover, several studies have reported about the distribution of CNHs in mice because biodistribution is one of the important factors of in vivo behavior when evaluating the biosafety of nanomaterials. Tahara et al. reported that CNHs intravenously administered biodistribution was influenced by chemical functionalization and CNHs accumulation in the lungs decreased with increased CNHs hydrophilicity. [44] Zang et al. also reported that biodistribution and excretion of CNHs in mice. CNHs accumulated mainly in the liver and spleen and a small amount of CNHs was excreted within the first few hours after injection, followed by much slower excretion rates obtained after 48 hours. [45] Previously, we have reported that the distribution of the implanted single-walled carbon nanotubes (SWCNTs) were observed by near-infrared (NIR) fluorescence imaging after SWCNTs were implanted between the periosteum and parietal bone of mice. [46] Fluorescence was not observed in other organs, including the liver, spleen, and lung, in whole-body imaging experiments whereas fluorescence was clearly observed in the cranial region even after 56 days. Then we suggested that locally implanted SWCNTs remain at the site of implantation and do not

accumulate in detectable quantities in other organs. For biological applications, it is necessary to investigate biological reactions for the long term, but these results suggested that the effects of MC/CNHs on cells and living bodies are relatively small.

Conclusion

MC could be adhered on CNHs prepared by mixing CNHs with MC aqueous solution. MC/as-CNHs were found to retain MC bacteriostatic properties. Therefore MC/CNHs would be advantageous for local drug delivery therapy such as peri-implantitis. We expect that our proof-of-concept study for local administration of MC/CNHs will promote future studies on the use of carbon nanomaterials in biomedicine and medicine.

Figures

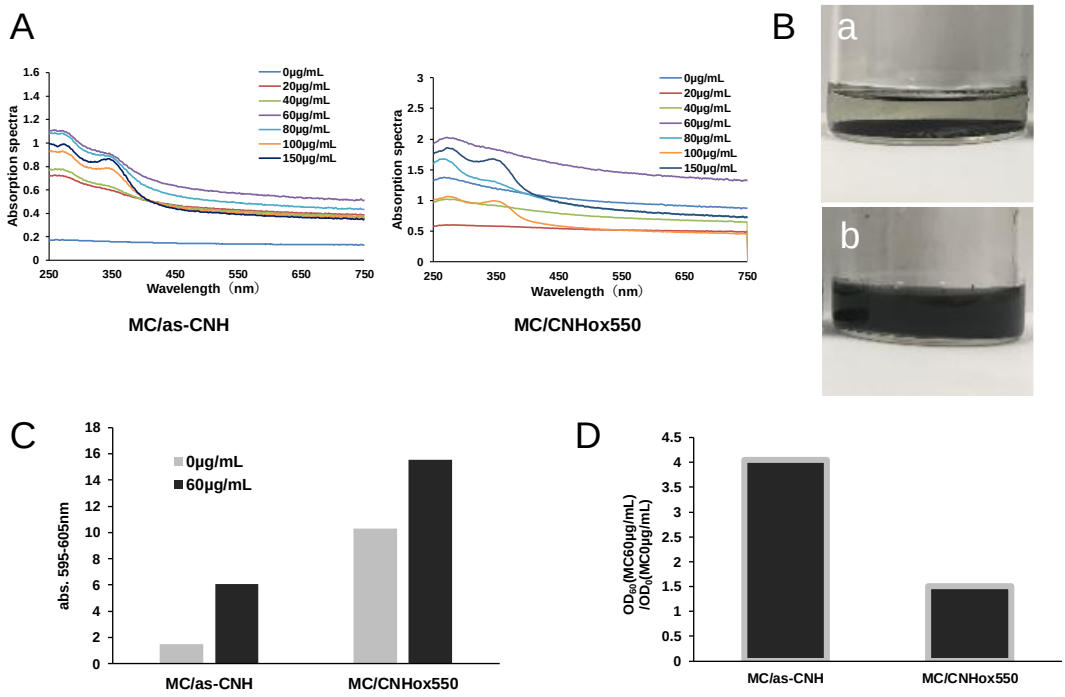

Fig.1 (A) Determination of dispersed CNH concentration in solution. (B) MC/CNHox550 before(a) and after(b) ultrasonication. (C)MC/CNHs were compared with the absorbance of the sum for 595 to 605 nm at MC concentration of 0μg/mL or 60μg/mL. (D)Dispersibility was determined by the absorbance OD60/OD0. It was defined that dispersibility improved when rate exceeded one.

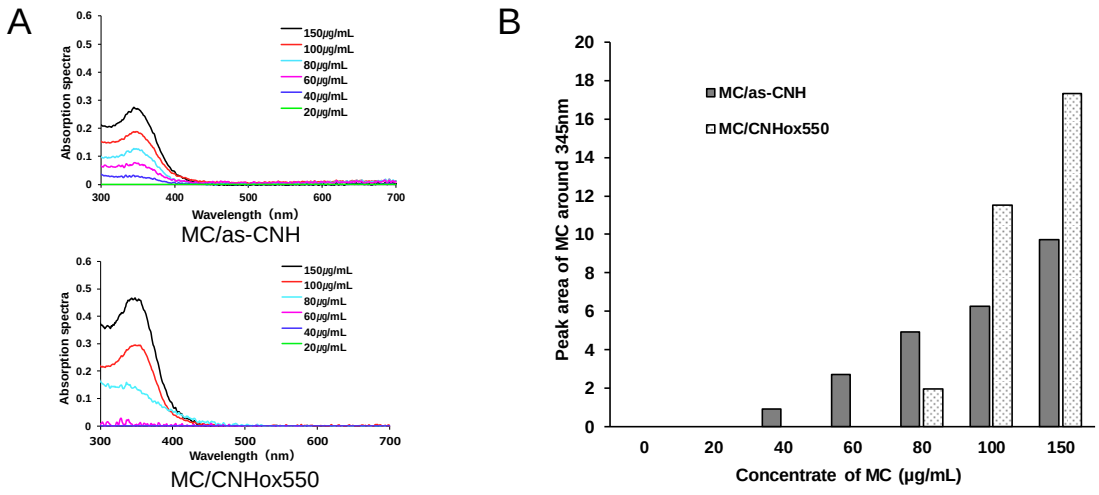

Fig. 2 (A) Absorbance plot when 20μg/mL was zero. (B) UV–VIS absorption spectra of MC/CNHs at 345nm with different MC concentrations.

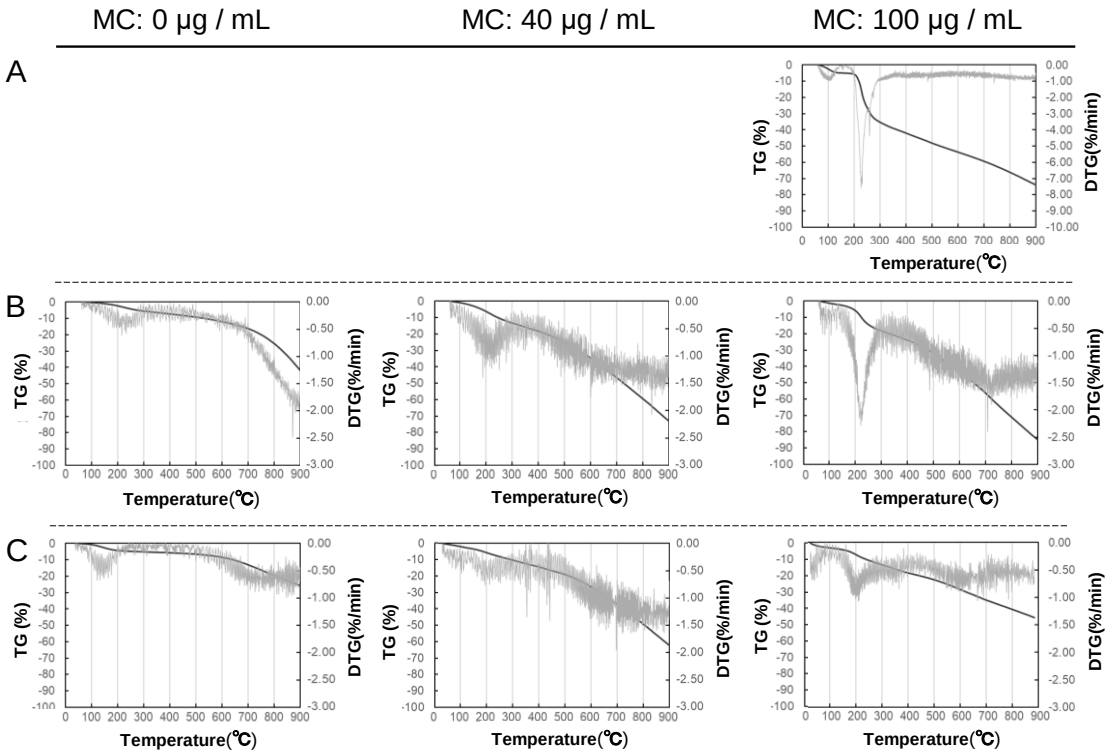

Fig. 3 TG/DTA of MC alone (A), MC/as-CNH (B), and MC/CNHox550 (C)

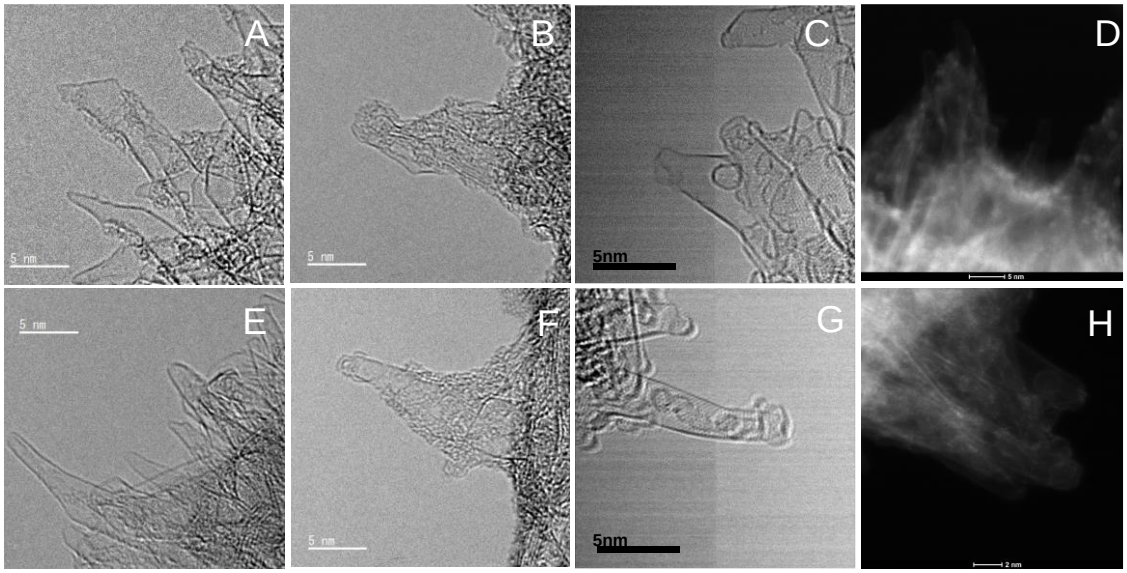

Fig. 4 200kV as-CNH(A), MC/as-CNH(B), HRTEM80kV MC/as-CNH(C), STEM80kV MC/as-CNH(D), 200kV CNHox550(E), MC/CNHox550(F), HRTEM80kV MC/CNHox550(G), STEM80kV MC/CNHox550(H)

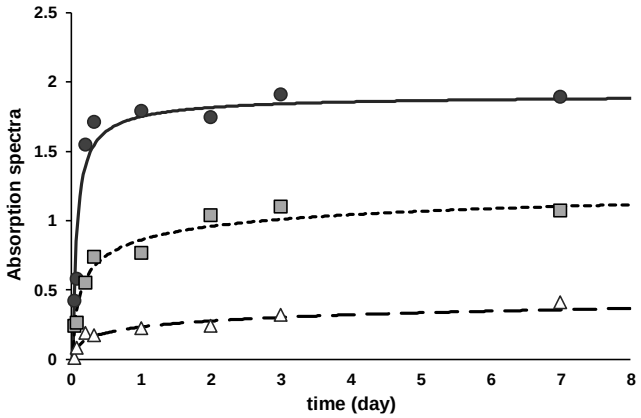

Fig. 5 Drug-release patterns compared for 7 days with total absorbance at 340-350nm. MC alone(●), MC/as-CNH(■), MC/CNHox550(△)

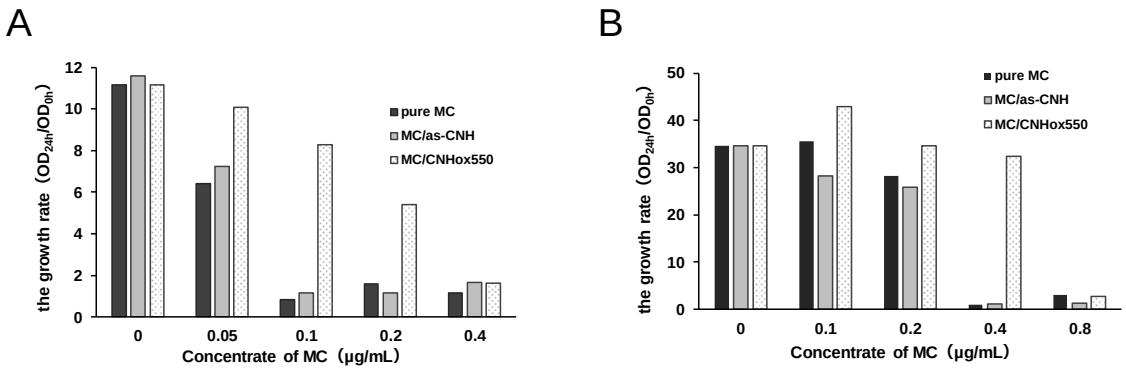

Fig. 6 Measurement of bacterial activity using turbidity with absorbance at 600nm. MC concentration was 0, 0.05, 0.1, 0.2, 0.4, 0.8 μg/mL. The growth rate was determined by the absorbance after 24hr/0hr. A.a.(A), S.m.(B)

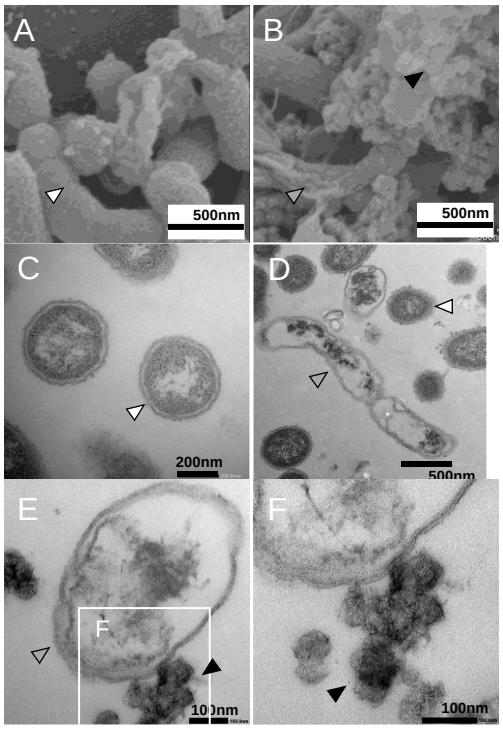

Fig. 7 SEM without CNHs(A), with MC/CNHox550(B), TEM MC (-) (C), MC (+) (D), MC/CNHox550(E)

White arrow is live bacteria, red arrow is dead bacteria, and black arrow is CNHs.

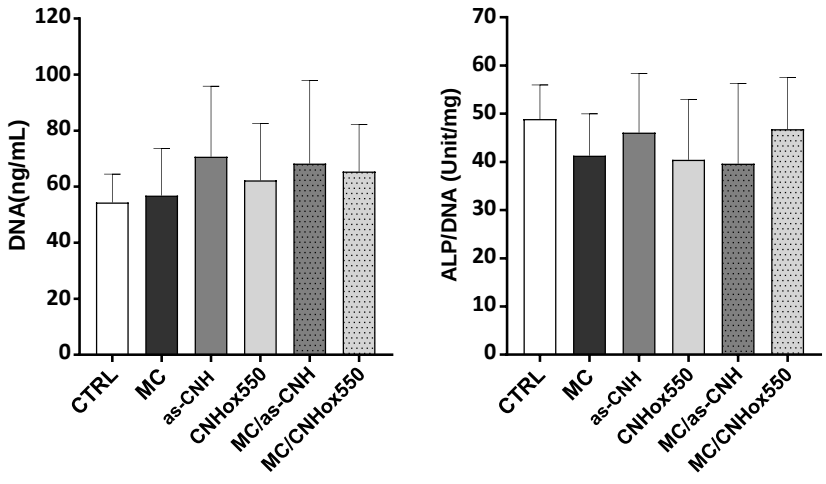

Fig. 8 ALP activity of MC3T3-E1 alone or cocultured with MC, as-CNH, CNHox550, MC/as-CNH, MC/CNHox550 after 7days.

References

1. Miyako E, Deguchi T, Nakajima Y, *et al.* Photothermic regulation of gene expression triggered by laser-induced carbon nanohorns. *Proc Natl Acad Sci U S A*. 109(19), 7523–7528 (2012).
2. Miyako E, Kono K, Yuba E, Hosokawa C, Nagai H, Hagihara Y. Carbon nanotube–liposome supramolecular nanotrains for intelligent molecular-transport systems. *Nat. Commun.* 3(1), 1226 (2012).
3. Battigelli A, Ménard-Moyon C, Bianco A. Carbon nanomaterials as new tools for immunotherapeutic applications. *J. Mater. Chem. B*. 2(37), 6144–6156 (2014).
4. Bianco A, Cheng HM, Enoki T, *et al.* All in the graphene family - A recommended nomenclature for two-dimensional carbon materials. *Carbon* . 65, 1–6 (2013).
5. Oliveira SF, Bisker G, Bakh NA, Gibbs SL, Landry MP, Strano MS. Protein functionalized carbon nanomaterials for biomedical applications. *Carbon*. 95, 767–779 (2015).
6. Cui X, Xu S, Wang X, Chen C. The nano-bio interaction and biomedical applications of carbon nanomaterials. *Carbon*. 138, 436–450 (2018).
7. Jiang BP, Zhou B, Lin Z, Liang H, Shen XC. Recent Advances in Carbon Nanomaterials for Cancer Phototherapy. *Chem. - A Eur. J.* 25(16), 3993–4004 (2019).
8. Mamathakumari M, Praveen Kumar D, Haridoss P, Durgakumari V, Shankar M V. Nanohybrid of titania/carbon nanotubes - Nanohorns: A promising photocatalyst for enhanced hydrogen production under solar irradiation. *Int. J. Hydrogen Energy*. 40(4), 1665–1674 (2015).
9. Attri P, Gaur J, Choi S, *et al.* Interaction studies of carbon nanomaterials and plasma activated carbon nanomaterials solution with telomere binding protein. *Sci. Rep.* 7(1), 1–14 (2017).
10. Türk S, Altınsoy I, Çelebi Efe G, Ipek M, Özacar M, Bindal C. 3D porous collagen/functionalized multiwalled carbon nanotube/chitosan/hydroxyapatite composite scaffolds for bone tissue engineering. *Mater. Sci. Eng. C*. 92(January), 757–768 (2018).

11. Shadjou N, Hasanzadeh M, Khalilzadeh B. Graphene based scaffolds on bone tissue engineering. *Bioengineered* . 9(1), 38–47 (2018).

12. Shrestha BK, Shrestha S, Tiwari AP, *et al.* Bio-inspired hybrid scaffold of zinc oxide-functionalized multi-wall carbon nanotubes reinforced polyurethane nanofibers for bone tissue engineering. *Mater. Des.*. 133, 69–81 (2017).

13. Dubey N, Bentini R, Islam I, Cao T, Castro Neto AH, Rosa V. Graphene: A Versatile Carbon-Based Material for Bone Tissue Engineering. *Stem Cells Int.* 2015, 18–23 (2015).

14. Hirata E, Uo M, Takita H, Akasaka T, Watari F, Yokoyama A. Development of a 3D collagen scaffold coated with multiwalled carbon nanotubes. *J. Biomed. Mater. Res. - Part B Appl. Biomater.* 90 B(2), 629–634 (2009).

15. Hirata E, Sakaguchi N, Uo M, *et al.* Transmission electron microscopic observation of cells cultured on multiwalled carbon nanotube-coated sponges. *J. Electron Microsc. (Tokyo).* 59(5), 447–450 (2010).

16. Hirata E, Uo M, Nodasaka Y, *et al.* 3D collagen scaffolds coated with multiwalled carbon nanotubes: Initial cell attachment to internal surface. *J. Biomed. Mater. Res. - Part B Appl. Biomater.* 93(2), 544–550 (2010).

17. Hirata E, Uo M, Takita H, Akasaka T, Watari F, Yokoyama A. Multiwalled carbon nanotube-coating of 3D collagen scaffolds for bone tissue engineering. *Carbon* . 49(10), 3284–3291 (2011).

18. Hirata E, Akasaka T, Uo M, Takita H, Watari F, Yokoyama A. Carbon nanotube-coating accelerated cell adhesion and proliferation on poly (L-lactide). *Appl. Surf. Sci.* 262, 24–27 (2012).

19. Iijima S, Yudasaka M. Nano-aggregates of single-walled graphitic carbon nano-horns. *Chem. Phys. Lett.* 309(August), 165–170 (1999).

20. Lacotte S, García A, Décossas M, *et al.* Interfacing Functionalized Carbon Nanohorns with Primary Phagocytic Cells. *Adv. Mater.* 20(12), 2421–2426 (2008).

21. Zhang M, Yang M, Bussy C, Iijima S, Kostarelos K, Yudasaka M. Biodegradation of carbon nanohorns in macrophage cells. *Nanoscale*. 7(7), 2834–2840 (2015).

22. Miyawaki J, Yudasaka M, Azami T, Kubo Y, Iijima S. Toxicity of Single-Walled Carbon Nanohorns. *ACS Nano*. 2(2), 213–226 (2008).

23. Vizuete M, Gómez-Escalonilla MJ, Barrejón M, *et al.* Synthesis, characterization and photoinduced charge separation of carbon nanohorn-oligothienylenevinylene hybrids. *Phys. Chem. Chem. Phys.* 18(3), 1828–1837 (2016).

24. He B, Shi Y, Liang Y, *et al.* Single-walled carbon-nanohorns improve biocompatibility over nanotubes by triggering less protein-initiated pyroptosis and apoptosis in macrophages. *Nat. Commun.* 9(1), 2393 (2018).

25. Lanone S, Andujar P, Kermanizadeh A, Boczkowski J. Determinants of carbon nanotube toxicity. *Adv. Drug Deliv. Rev.* 65(15), 2063–2069 (2013).

26. Murata K, Kaneko K, Steele WA, *et al.* Molecular potential structures of heat-treated single-wall carbon nanohorn assemblies. *J. Phys. Chem. B*. 105(42), 10210–10216 (2001).

27. Murakami T, Ajima K, Miyawaki J, Yudasaka M, Iijima S, Shiba K. Drug-loaded carbon nanohorns: adsorption and release of dexamethasone in vitro. *Mol. Pharm.* 1(6), 399–405 (2004).

28. Ajima K, Yudasaka M, Murakami T, Maigné A, Shiba K, Iijima S. Carbon nanohorns as anticancer drug carriers. *Mol. Pharm.* 2(6), 475–480 (2005).

29. Xu J, Yudasaka M, Kouraba S, Sekido M, Yamamoto Y, Iijima S. Single wall carbon nanohorn as a drug carrier for controlled release. *Chem. Phys. Lett.* 461(4–6), 189–192 (2008).

30. Kasai T, Matsumura S, Iizuka T, *et al.* Carbon nanohorns accelerate bone regeneration in rat calvarial bone defect. *Nanotechnology*. 22(6), 065102 (2011).

31. Hirata E, Miyako E, Hanagata N, *et al.* Carbon nanohorns allow acceleration of osteoblast differentiation via macrophage activation. *Nanoscale*. 8(30), 14514–14522 (2016).

32. Sadowsky SJ. Occlusal overload with dental implants: a review. *Int. J. Implant Dent.* 5(1) (2019).

33. Sanz M, Noguerol B, Sanz-Sanchez I, *et al.* European Association for Osseointegration Delphi study on the trends in Implant Dentistry in Europe for the year 2030. *Clin. Oral Implants Res.* 30(5), 476–486 (2019).

34. Roos-Jansåker AM, Renvert H, Lindahl C, Renvert S. Nine- to fourteen-year follow-up of implant treatment. Part III: Factors associated with peri-implant lesions. *J. Clin. Periodontol.* 33(4), 296–301 (2006).

35. Koldsland OC, Scheie AA, Aass AM. Prevalence of Peri-Implantitis Related to Severity of the Disease With Different Degrees of Bone Loss. *J. Periodontol.* 81(2), 231–238 (2010).

36. Francetti L, Cavalli N, Taschieri S, Corbella S. Ten years follow-up retrospective study on implant survival rates and prevalence of peri-implantitis in implant-supported full-arch rehabilitations. *Clin. Oral Implants Res.* 30(3), 252–260 (2019).

37. Lee J Bin, Kweon HHI, Cho HJ, Kim CS, Kim YT. Characteristics of local delivery agents for treating peri-implantitis on dental implant surfaces: A preclinical study. *J. Oral Implantol.* 45(2), 116–126 (2019).

38. Garrido-Mesa N, Zarzuelo A, Gálvez J. Minocycline: Far beyond an antibiotic. *Br. J. Pharmacol.* 169(2), 337–352 (2013).

39. Park JB. Effects of doxycycline, minocycline, and tetracycline on cell proliferation, differentiation, and protein expression in osteoprecursor cells. *J. Craniofac. Surg.* 22(5), 1839–1842 (2011).

40. Azami T, Kasuya D, Yuge R, *et al.* Large-scale production of single-wall carbon nanohorns with high purity. *J. Phys. Chem. C.* 112(5), 1330–1334 (2008).

41. Fan J, Yudasaka M, Kasuya D, *et al.* Micrometer-sized graphitic balls produced together with single-wall carbon nanohorns. *J. Phys. Chem. B.* 109(21), 10756–10759 (2005).

42. Fan J, Yudasaka M, Miyawaki J, Ajima K, Murata K, Iijima S. Control of hole opening in single-wall carbon nanotubes and single-wall carbon nanohorns using oxygen. *J. Phys. Chem. B*. 110(4), 1587–1591 (2006).

43. Nanci A, Zalzal S, Gotoh Y, McKee MD. Ultrastructural characterization and immunolocalization of osteopontin in rat calvarial osteoblast primary cultures. *Microsc. Res. Tech.* 33(2), 214–231 (1996).

44. Tahara Y, Miyawaki J, Zhang M, *et al.* Histological assessments for toxicity and functionalization-dependent biodistribution of carbon nanohorns. *Nanotechnology*. 22(26) (2011).

45. Zhang M, Jasim DA, Ménard-Moyon C, *et al.* Radiolabeling, whole-body single photon emission computed tomography/computed tomography imaging, and pharmacokinetics of carbon nanohorns in mice. *Int. J. Nanomedicine*. 11, 3317–3325 (2016).

46. Hirata E, Yudasaka M, Ushijima N, *et al.* Fate of Carbon Nanotubes Locally Implanted in Mice Evaluated by Near-Infrared Fluorescence Imaging: Implications for Tissue Regeneration. *ACS Appl. Nano Mater.* 2(3), 1382–1390 (2019).